Yearly variation and annual cycle of total column ozone over New Delhi (29°N, 77°E), India and Halley Bay (76°S, 27°W), British Antarctic Survey Station and its effect on night airglow intensity of OH(8, 3) for the period 1979–2005

P K JANA[1,*], D K SAHA[2] and D SARKAR[3]

[1]*Department of Chemistry, Institute of Education (P. G) for Women, Chandernagore, Hooghly 712 138, West Bengal, India.*
[2]*Department of Chemistry, Dinabandhu Mahavidyalaya, Bangaon, North 24 Parganas 743 235, West Bengal, India.*
[3]*Department of Chemistry, Howrah Zilla School, Howrah 711 101, West Bengal, India.*
[*]*Corresponding author. e-mail: pkjjngl@yahoo.co.in*

A critical analysis made on the long-term monthly, seasonal, yearly variation and annual cycle of total column ozone (TCO) concentration at New Delhi (29°N, 77°E), India and Halley Bay (76°S, 27°W), a British Antarctic Service Station reveals more decline in yearly mean ozone concentration at Halley Bay than at New Delhi from 1979 to 2005. The nature of variations of monthly mean TCO during the months of August and September was the most identical with that of yearly mean ozone values at New Delhi and Halley Bay, respectively, for the same period. Annual cycles of TCO over these stations are completely different for the above period. The effect of O_3 depletion on night airglow emission of OH(8, 3) line at New Delhi and Halley Bay has been studied. Calculations based on chemical kinetics show that the airglow intensity of OH(8, 3) has also been affected due to the depletion of O_3 concentration. The yearly variations and annual cycle of intensities of OH(8, 3) line for the above two stations are depicted and compared. It has been shown that the rate of decrease of intensity of OH(8, 3) line was comparatively more at Halley Bay due to dramatic decrease of Antarctic O_3 concentration.

1. Introduction

In the upper atmosphere, where the densities of air molecules are relatively small and more high energy photons are sufficient to produce excited species, many constituents fluoresce or chemiluminescence. This self-luminescence of the upper atmosphere called the airglow emission (Midya and Midya 1993) that occurs in all latitude (deMesnes *et al.* 2011) comprises the light of the wavelengths ranging from the far UV to near IR (Hargreaves 1992; Gombosi 2004). The airglow emissions do exist during both the day and night including twilight also. The mechanism for excitation involves photo-ionization, photoelectron excitation and chemical excitation. Photo-ionization, photoelectron excitation and chemical excitation are active during daytime, while the chemical excitation is the only source for the night-time airglow emission apart from the small

Keywords. Ozone depletion; airglow emission; excitation mechanism; intensity.

contribution from cosmic rays. The lifetime of the excited species ranges from milliseconds to minutes depending upon the altitudes from which they emanate. Green and red lines of oxygen, yellow lines of sodium and OH bands are the main emissions during day, twilight and night time. Meinel (1950a) first identified rotational–vibrational band of OH airglow emission. Meinel (1950a, 1950b, 1950c) discovered various vibration–rotation bands of the OH radical in the night airglow. These are known as the Meinel (M) bands, viz., OH M(7, 4) band, OH M(6, 3) band, OH M(3, 1) band, OH M(4, 2) and OH(5, 3) R heads. OH M(7, 4) band, OH M(6, 3) band, OH M(3, 1) band, OH M(4, 2) band and OH M(5, 3) band have been identified near 7530, 8744, 6169, 6503, and 6165 cm^{-1}, respectively. OH(8, 3) is the other important emission of airglow spectrum. Takahashi *et al.* (1974) identified OH(8, 3) band airglow emission at latitude of 23°S. They also reported that nocturnal variation of intensity was correlated with that of a rotational temperature. Krassovsky and Shagaev (1974) observed the wave-like propagation of disturbances of rotational temperature of OH(8, 3). Takahashi *et al.* (1977) studied the diurnal and seasonal variation of intensity of OH(8, 3) emission from 1972 to 1974. It showed a significant seasonal effect. The OH(8, 3) emission was found to increase slightly during magnetic disturbances. The proposed excitation mechanism (Bates and Nicolet 1950) of OH(8, 3) line indicates that the intensity of OH(8, 3) line is affected with the variation of ozone concentration.

Ozone, though a very minor atmospheric constituent, plays an important role to control the chemical kinetics of troposphere, stratosphere and mesosphere. The global ozone assessment confirms that ozone is declining everywhere in smaller amount (Bojkov 1992). But Farman *et al.* (1985) first reported that dramatic decrease of ozone concentration takes place at Antarctica during spring time causing an ozone hole. Afterwards, it was verified by different investigators all over the world (Midya and Jana 2002).

Conventionally, it is assumed that there is an ozone hole when the ozone abundance is $\leq$220 Dobson units (D U) (1 DU = 0.001 atm cm) in a specific geographic place (WMO 2002). The 1997 monthly averaged column ozone from the total ozone mapping spectrometer (TOMS) is up to 25 DU lower than the TOMS climatological mean (1979–1996) and up to 20 DU below the previous record low values (Cordero and Nathan 2002). Kerr (1998) reported that the 1998 Antarctic ozone hole is the biggest one ever observed. Average area of ozone hole was 25.3×10^6 km^2 in September and 20.6×10^6 km^2 in October 1998. The area of Antarctic ozone hole (area of $O_3 < 220$ DU) increased (Uchino *et al.* 1999) steadily from 1979 to 1998 and the 2000 ozone hole was the largest on record (Bodeker *et al.* 2002). Averaged area of the Antarctic ozone hole, determined by the area enclosed by the 220 DU total ozone contour, increased (Madrigal and Peraza 2005) from 2.6×10^6 to 25.8×10^6 km^2 for the month of September and from 2.7×10^6 to 16.7×10^6 km^2 for the month of October, during 1982–2003. Several theories have been proposed for the Antarctic ozone hole. Chemical, dynamical and natural theories are mainly important and are explained in an earlier publication (Jana and Nandi 2005). If ozone hole is created at any place in the atmosphere, O_3 concentration also decreases in other regions due to atmospheric diffusion and circulation (Jana and Nandi 2005).

Measurement of airglow emission can be used as an important tool in studying the behaviour of the ionosphere and the upper atmosphere basically on the dynamical–photochemical processes that control the species composition and energy balance (Krasnopolsky 1986; Haider *et al.* 1992; Slanger *et al.* 2001). OH airglow emissions can be used as tracers of gravity wave (GW) that play an essential role in determining the global circulation and thermal balance of the atmosphere. A realistic GW parameterization is important for accurate atmospheric model. Dynamic control of OH altitude/temperature at high latitudes was supported by the anti-correlation between OH peak altitude and temperature found in SABER (Sounding of the Atmosphere using Broadband Emission Radiometry) data (Winick *et al.* 2009) and also between OH peak altitude and meridional wind strength (Dyrland *et al.* 2010). Measurement of OH airglow can be used to derive atomic hydrogen concentration if ozone density is known (Mlynczak *et al.* 1998) and the OH rotational temperature near the mesopause (Lowe and Turnbull 1995). The OH airglow emission can extensively be used for studying atmospheric temperature variation at mesospheric region (Greet *et al.* 1998; Bittner *et al.* 2000). The airglow OH(8-3) and (6-2) band rotational temperatures were measured and compared using two scanning photometer at Cachoeira Paulista (23°S, 45°W) in 1999. The rotational temperature were obtained from the ratio between the $P_1(5)$ and $P_1(3)$ in the case of (8-3) band and $P_1(4)$ and $P_1(2)$ lines for the (6-2) band. It was shown that both the temperature did agree well (Wrasse *et al.* 2004).

Airglow emission can be influenced by atmospheric parameters including temperature, vertical advection, diffusion and some chemical species. Moreover, its temporal and spatial distributions are often modulated by dynamical perturbation such as gravity waves, planetary waves, tides and

so on. Stratospheric sudden warming (SSW), the most important event in the mid-winter polar stratosphere can perturb atmospheric temperature, winds and distribution of several atmospheric chemical constituents in the middle atmosphere (Sathiskumar and Sridharan 2009; Funke *et al.* 2010). Therefore, influence of variation of total column ozone on OH airglow emission is an important approach for investigating the coupling between stratosphere and mesosphere-lower thermosphere (MLT) region (Gao *et al.* 2011). Wiens and Weill (1973) on analysis of the diurnal, annual and solar cycle variations in OH nightglow reported that the diurnal variation patterns altered with latitude and season and OH nightglow intensity followed the solar activity. Batista *et al.* (1994) showed that the OH(9, 4) band intensity had a positive correlation with the $F10.7$ index. Abreu and Yee (1989) on the basis of the seasonal variations in the OH(8, 3) nightglow emission pointed out that there was a strong semi-annual oscillation with maxima near the equinoxes in the OH nightglow. Marsh *et al.* (2006) mentioned that the OH nightglow was stronger than the OH day glow. Shephered *et al.* (2006) showed that a 1% increase in temperature led about 4% increase in OH emission and OH emission was linearly sensitive to atomic oxygen concentration on the bottom side of the atomic oxygen layer.

In this paper, the nature of variations of monthly, yearly and seasonal total column ozone (TCO) over New Delhi and Halley Bay has been presented from 1979 to 2005. The most and the least identical monthly and seasonal variations with that of yearly TCO have been identified for these stations. Annual cycle of monthly TCO over these two stations has also been depicted. From the excitation mechanism OH(8, 3) airglow emission, the volume emission rate for different altitudes are computed. From the volume emission rate curve, the intensity of OH(8, 3) has been calculated for the year 1979. Following this process, the intensity of the same line over two stations, namely, New Delhi, India which has comparatively less depletion in ozone concentration and Halley Bay (76°S, 27°W), a British Antarctic Survey station which has comparatively much more depletion in ozone concentration, have been calculated for other years, considering the fluctuation percentages of O_3 concentrations assuming that the variation of OH intensity is unaffected by the density of atomic hydrogen. The nature of different type of variations of TCO and intensities of OH(8, 3) is compared over these two stations because the stations are associated with distinctly different rates of ozone depletion without considering the semiannual oscillation (SAO), annual oscillation (AO) and quasi-biennial oscillation (QBO). In our previous publications (Jana and Nandi 2006; Jana *et al.* 2011), effect of long term TCO on intensities of Na 5893 Å nightglow line and lithium 6708 Å over Dumdum (22.5°N, 88.5°E) and Varanasi (25°N, 83°E) had been presented and compared with that at Halley Bay (76°S, 27°W), respectively which showed same type of excitation mechanisms of sodium and lithium airglow emissions having different types of their importance in mesosphere. In case of OH(8, 3) airglow emission, the excitation mechanism and the role of OH(8, 3) which is stated above are completely different from the sodium and lithium airglow emission.

2. Data and analysis

Total column ozone densities of different stations have been obtained from the website http://jwocky.gsfc.nasa.gov (Jana *et al.* 2010a, 2010b). Monthly mean ozone densities have been calculated from daily average value of ozone in DU for the stations, namely, New Delhi and Halley Bay. The yearly mean ozone densities have been calculated from monthly average value of ozone in DU. The mean ozone for December, January and February (DJF) provides winter (summer) ozone, March, April and May (MAM) constitute pre-monsoon (fall) values, June, July and August (JJA) make monsoon (winter) values and September, October and November (SON) comprise post-monsoon (spring) values for the station New Delhi (Halley Bay), respectively. Total ozone data has been measured by the satellites Nimbus-7 Total Ozone Mapping Spectrometer (TOMS), Earth probe TOMS and Ozone Monitoring Instrument (OMI). TOMS and OMI provide high resolution daily global information about the total ozone content of the atmosphere by measuring ultraviolet sunlight backscattered from the ground. TCO in this study includes retrievals from Nimbus 7 (November 1978 to May 1993) and Earth probe (July 1996 to present) total ozone mapping spectrometer (TOMS). Data from HALOE (halogen occultation experiment) are used in this first method to extend the vertical span of MLS (highest pressure level 46 hPa) using simple regression. This assimilation enables high resolution daily maps of tropospheric and stratospheric ozone which is not possible from solar occultation measurements alone, such as from HALOE or Stratospheric Aerosols and Gas Experiment (SAGE) (Jana *et al.* 2012).

3. Results and discussions

The proposed excitation mechanisms of OH(8, 3) band are as follows:

1. Bates–Nicolet mechanism (Bates and Nicolet 1950)

$$O + O_2 + M \xrightarrow{K_1} O_3 + M, \quad (1)$$

$$O_3 + H \xrightarrow{K_2} O_2 + OH^* (3.32\,ev), \quad (2)$$

$$OH^* \xrightarrow{Avv'} OH + hv, \quad (3)$$

where $K_1 = 1.5\times10^{-34} \exp(445/T)$ cm^6 S^{-1} (Stuhl and Niki 1971) and $K_2 = 1.5 \times 10^{-12}\sqrt{T}$ cm^3 S^{-1} (Nicolet 1970).

2. Breig mechanism (Breig 1970)

$$H + M + O_2 \xrightarrow{K_3} HO_2 + M, \quad (4)$$

$$HO_2 + O \xrightarrow{K_4} OH^* + O_2, \quad (5)$$

where $K_3 = 3.3 \times 10^{-33} \exp(800/T)$ cm^6 S^{-1} (Gattinger 1971) and $K_4 = 1.5\times10^{-12}\sqrt{T}$ cm^3 S^{-1} (Gattinger 1971).

3. Krassovsky mechanism (Krassovsky 1956)

$$O_2 + O + M \xrightarrow{K_5} O_3 + M, \quad (6)$$

$$O + O_3 \xrightarrow{K_6} O_2^* + O_2^*, \quad (7)$$

$$O_2^* + H \xrightarrow{K_7} OH^* + O, \quad (8)$$

where $K_5 = 1.5\times10^{-32}$ cm^6 S^{-1} (Midya *et al.* 1998) and $K_7 = 10 \times 10^{-10}$ cm^3 S^{-1} (Midya *et al.* 1998). K_1, K_2, K_3, K_4, K_5, K_6 and K_7 are all reaction rate constants. Midya *et al.* (1998) have established that Bates–Nicolet mechanism is the predominant and appropriate excitation mechanism of OH emission.

According to Bates–Nicolet mechanism, ignoring quenching terms, the volume emission rate of OH* is given by:

$$n(OH^*) = K_2 [O_3] [H] \quad (9)$$

So, the volume emission rate of OH(8, 3) band will be as follows:

$$Q^*_{OH} = A_{8,3} K_2 [O_3] [H] / \sum Avv'. \quad (10)$$

where Avv′ is the Einstein transition probability from vibrational level v to v′.

$$A_{8,3} = 0.0296\,S^{-1} \quad (11)$$

$$\sum Avv' = 13.5 \text{ (Midya } et\ al. \text{ 1998)}. \quad (12)$$

The Einstein A-coefficients associated with the OH* vibrational emissions have been measured in the laboratory (Nelson *et al.* 1990). Uncertainties regarding the quenching lifetimes and the rate constants for the reactions with atomic O remain fairly large (Mlynczak *et al.* 1998) and make the interpretation of the airglow feature difficult (Llewellyn *et al.* 1978).

Using the number densities of O_3 and H, the volume emission rates of OH(8, 3) band for different altitudes have been calculated with the help of the equation (10). It attains maximum value at an altitude of 80 km. Altitudinal number densities of O_3 and H and volume emission rates of OH(8, 3) band have been shown in table 1. Intensity has then been calculated from the volume emission rate curve with the help of the following equation:

$$\text{Intensity} = \frac{1}{2} \times \text{layer thickness} \times \text{peak volume emission rate}. \quad (13)$$

The value of layer thickness was 14.8 km and peak volume emission rate was 46×10^2 cm^{-3} s^{-1} for normal volume emission rate curve shown in figure 1. Thus, the intensity of OH(8, 3) band became 34.04 KR (KiloRayleigh) (1R = 1.0×10^5 cm^{-2} s^{-1}). The number densities of H and O_3 have been taken from Jacchia (1977). The OGO-satellite mass spectrometer launched in 1969 provided the first measurements of the densities of N_2, O and He in the thermosphere. The observed variations in composition did not agree with Jacchia model. Accuracy may be improved with the corresponding data produced from MSIS (Mass Spectrometer and incoherent Scatter) model for various geographical, temporal and solar conditions, but pattern of variations of yearly, seasonal and annual cycle of OH intensities would be unaltered. The latest model, MSIS-86 was chosen for CIRA (COASPER International Reference) 1986. The database for MSIS-86 consists of composition, temperature and density data with *in situ* thermospheric measurements as well as rockets and ground based scatter stations (Marcos 1987). Gao *et al.* (2010) had also calculated the mean OH nightglow emission rate at the altitude of 88 km, the temperature and $[O_3]$ at 88 km which were observed by SABER, but they did not use [O] and [H] data measured by SABER because of large errors. They found that the distribution of the OH nightglow emission rate at 88 km, the peak emission rate (V_{max}), intensity (I) and $[O_3]$ are similar to one another. Thus, they also concluded that the seasonal variations of temperature, [O], and $[O_3]$ played an important role in the seasonal variation of OH nightglow emission, V_{max} and I. The TIMED (Thermosphere, Ionosphere, Mesosphere, Energetics, and Dynamics) satellite was launched on 7 December. The height of the TIMED circular orbit is about 625 km and the inclination is 74.1°. The SABER, one of the four instruments onboard the TIMED satellite directly measures atmospheric emissions, such as OH airglow emission, O_2 airglow emission and NO airglow emission over a broad spectral range using a multichannel infrared

Table 1. *Volume emission rates of OH(8, 3).*

Altitude (km)	Number densities (atoms/cc)					Volume emission rates(Q) of OH(8, 3)		
	$n(O_3) \times 10^{-8}$	$n(H) \times 10^{-8}$	$QOH(8, 3) \times 10^{-2}$	$n(O_3) \times 10^{-8}$ New Delhi	$n(O_3) \times 10^{-8}$ Halley Bay	Normal $cm^{-3}\ s^{-1}$	New Delhi $cm^{-3}\ s^{-1} \times 10^{-2}$	Halley Bay $cm^{-3}\ s^{-1} \times 10^{-2}$
75	3.2	0.51	7.25	3.33	3.76	7.25	7.54	8.52
76	2.8	2.1	26.2	2.91	3.29	26.2	27.25	30.79
77	2.5	3.7	41.2	2.6	2.94	41.2	42.85	48.41
78	2.1	5.4	50.5	2.18	2.47	50.5	52.52	59.34
79	1.8	7	56.1	1.87	2.12	56.1	58.34	65.92
80	1.4	8.6	53.6	1.46	1.65	53.6	57.74	62.98
81	1.3	8.3	48	1.35	1.53	48	49.92	56.4
82	1.2	7.9	42.2	1.25	1.41	42.2	43.89	49.59
83	1.16	7.6	39.2	1.21	1.36	39.2	40.77	46.06
84	1.08	7.2	34.6	1.12	1.27	34.6	35.98	40.65
85	1	6.9	30.7	1.04	1.18	30.7	31.93	36.07
86	1.02	5.9	26.8	1.06	1.2	26.8	27.87	31.49
87	1.04	5.1	23.6	1.08	1.22	23.6	25.45	27.73
88	1.06	4.1	19.3	1.1	1.25	19.3	20.07	22.68
89	1.08	3.2	15.4	1.12	1.27	15.4	16.02	18.09
90	1.1	2.3	11.3	1.14	1.29	11.3	11.75	13.28

radiometer and indirectly measures atmospheric parameters, such as temperature, atmospheric density, ozone density, atomic oxygen density and so on.

Variations of yearly mean ozone concentrations at New Delhi and Halley Bay have been presented in figures 2 and 3, respectively, from 1979 to 2005. The nature of variations of ozone concentrations for each month for different years has been compared with the variation of yearly mean ozone concentrations. It has been observed that the variations of ozone concentrations for all months and variation of yearly mean ozone values followed nearly the same trend. The nature of variation of mean ozone values during the month of August from 1979 to 2005 was the most identical with the variation of yearly mean ozone values for the same period and the variation of mean ozone values during the month of December was the least identical with the variation of yearly mean ozone values for the same period at New Delhi. It has also been verified by the value of coefficient of correlation as depicted in figure 4 that depicts the variation of correlation coefficients with months at New Delhi (29°N, 77°E) and at Halley Bay (76°S, 27°W) from 1979 to 2005. The coefficient of correlation between August ozone mean values with yearly mean values was the maximum (0.82). It was the minimum for December ozone mean values (0.35). The yearly mean ozone concentration as well as the concentrations of ozone for every month was gradually decreasing from 1979 to 2005 at different rates at New Delhi. The rate of yearly mean ozone depletion was 0.3629 DU per year. It was 0.2102 and 0.8053 DU per year for the months of August and December, respectively. Therefore, the variation of August concentration of ozone mostly controlled the variation of annual TCO over New Delhi from 1979 to 2005 as the rate of ozone fall in August from 1979 to 2005 was the closest to that of annual TCO.

But in case of Halley Bay, the nature of variation of mean ozone values during the month of September from 1979 to 2005 was the most identical with the variation of yearly mean ozone values for the same period and the variation of mean ozone values during the month of April was the least identical with the variation of yearly mean ozone values for the same period. It has also been verified by the value of coefficient of correlation as shown in figure 4. The coefficient of correlation between September ozone mean values with yearly mean values was the maximum (0.97). It was the minimum for April ozone mean values (0.51). The yearly mean ozone concentration as well as the concentrations of ozone for every month was gradually decreasing from 1979 to 2005 at different rates. The rate of yearly mean ozone

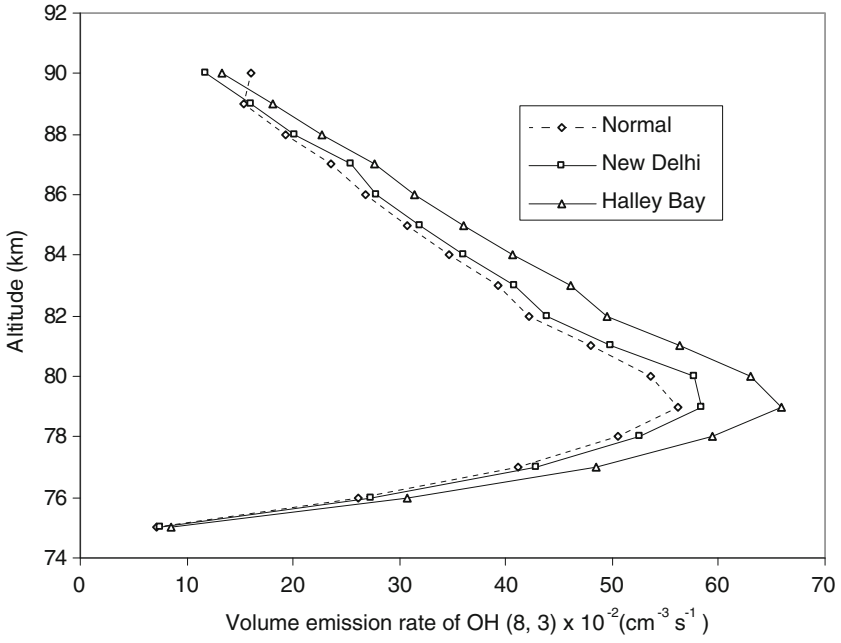

Figure 1. Altitudinal variations of volume emission rates of OH(8, 3) band at New Delhi (29°N, 77°E) and at Halley Bay (76°S, 27°W).

depletion was 2.684 DU per year. It was 4.7434 and 1.0914 DU per year for the months of September and April, respectively. So, the variation of yearly mean TCO over Halley Bay was controlled by that of September ozone values.

Seasonal variations of ozone densities at New Delhi reveal the most identical variation in DJF (winter) and least identical variation in SON

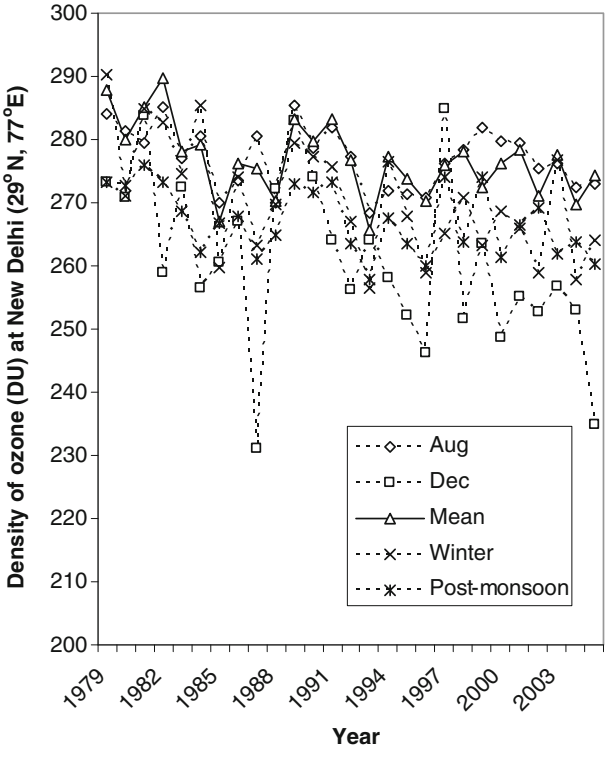

Figure 2. Variation of ozone concentration at New Delhi (29°N, 77°E) from 1979 to 2005.

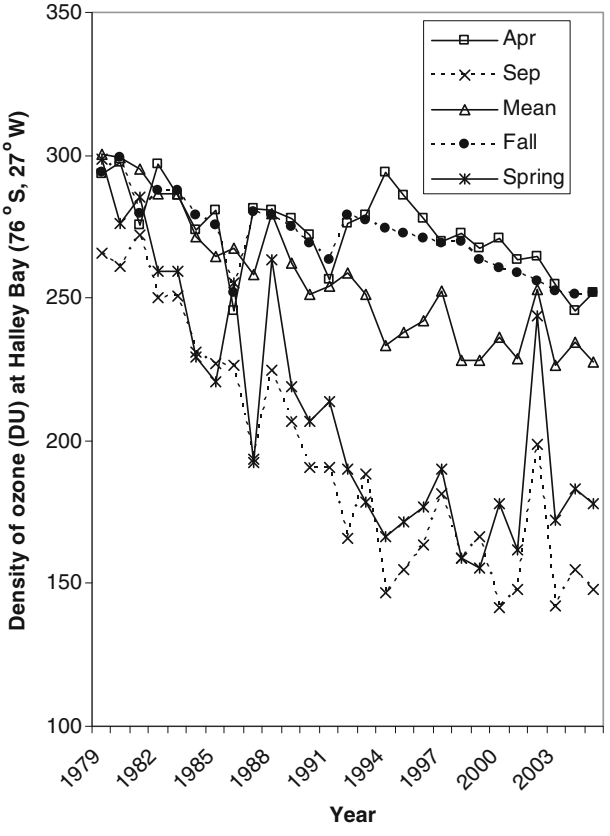

Figure 3. Variation of ozone concentration at Halley Bay (76°S, 27°W) from 1979 to 2005.

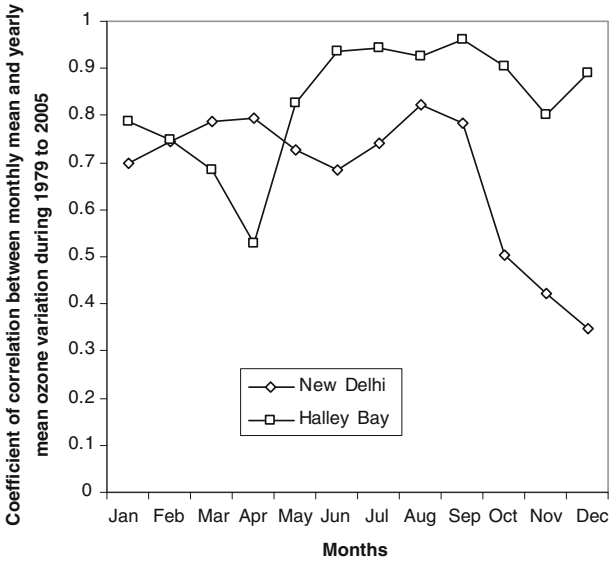

Figure 4. Variation of correlation coefficients with months at New Delhi (29°N, 77°E) and at Halley Bay (76°S, 27°W) from 1979 to 2005.

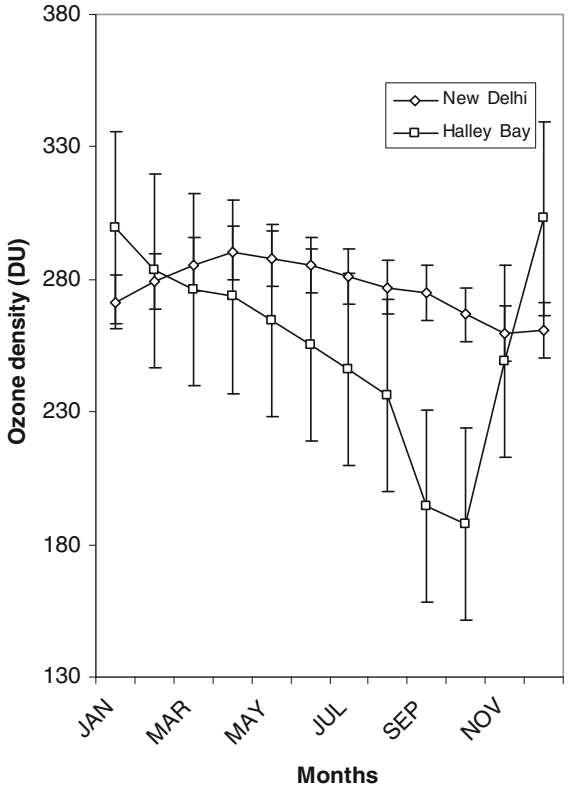

Figure 5. Annual cycle of ozone concentration at New Delhi (29°N, 77°E) and Halley Bay (76°S, 27°W).

(post-monsoon) with yearly mean variation. The rate of ozone depletion was 0.0763 and 0.028 DU per year in winter and post-monsoon, respectively. But, in case of Halley Bay, the most identical seasonal variations of ozone were observed in SON (spring), while the least identical seasonal variation in MAM (fall) with yearly mean ozone variation. The rate of ozone decline was 0.7174 and 0.159 DU per year in spring and fall, respectively.

Annual cycle of ozone concentrations for the stations at New Delhi and Halley Bay for the period 1979–2005 have been shown in figure 5, respectively. At New Delhi, ozone concentration attained the maximum value for the months of June and July. The minimum ozone concentration occurred for the months of December and January. Ozone concentration gradually increased from the month of January, attained its maximum for the period of June and July, then gradually decreased and reached its minimum value for the month of December.

In case of Halley Bay, ozone concentration attained the maximum value for the months of December and January. The minimum ozone concentration occurred at the months of September and October. Maximum ozone concentration occurred during the month of January, then gradually decreased, attained minimum for the month of September–October and then gradually increased. At both the stations, annual cycle of ozone densities for every year and their mean annual cycle followed nearly the identical variations.

Equation (10) clearly reveals that the volume emission rate of OH(8, 3) band is directly proportional to the concentrations of H and ozone ($O_3 + H \rightarrow OH^* + O_2$) with the reaction rate increasing with increasing temperature. O_3 is produced from the reaction $O + O_2 + M \rightarrow O_3 + M$ and is destroyed mostly by the reaction $O_3 + H^* \rightarrow OH^* + O_2$ and $O + O_3 \rightarrow O_2 + O_2$. The destruction of ozone due to the reaction with H is larger than the reaction with O by several orders of magnitude below 95 km (Xu *et al.* 2010). So, the contribution of producing OH airglow is somewhat nullified by the destruction of O_3 that produces OH airglow. The production of O_3 and consequent OH nightglow emission at mesosphere are proportional to the atomic oxygen density, thus OH airglow emission is influenced by atomic oxygen, ozone densities and also by atmospheric temperature. Ward (1999) reported that the OH nightglow is approximately proportional to the volume mixing ratio of O. Marsh *et al.* (2006) indicated that the transport of O is responsible for the annual cycle of the SABER OH emissions at higher latitudes. Xu *et al.* (2010) pointed out that the SABER OH nightglow brightness and temperature near the equator were positively correlated below about 94 km and negatively correlated above. The concentration of ozone in stratosphere varies in considerable amount from year to year, as well as from month to month. This stratospheric variation of ozone may influence the mesospheric altitudinal concentration of ozone. On the basis of recent study on the

Table 2. *Yearly variation of intensity of OH(8, 3) at New Delhi and Halley Bay.*

Year	Mean O_3 (DU) at New Delhi	O_3 fluctuation % from mean at New Delhi	Mean O_3 (DU) at Halley Bay	O_3 fluctuation % from mean at Halley Bay	Peak volume emission rate OH(8, 3) at New Delhi cm^{-3} $\mathbf{s}^{-1}$	Peak volume emission rate OH(8, 3) at Halley Bay cm^{-3} s^{-1}	Intensity of OH(8, 3) line at New Delhi KR	Intensity of OH(8, 3) line at Halley Bay KR
1979	287.81	4.007	300.54	17.5	58.34	65.92	35.4	39.99
1980	280.13	1.225	299.48	17.08	56.79	65.68	34.46	39.85
1981	285.11	3.03	294.94	15.31	57.79	64.69	35.07	39.25
1982	289.69	4.687	286.14	11.87	58.73	62.76	35.64	38.08
1983	278.07	0.487	286.56	12.03	56.37	62.85	34.21	38.14
1984	279.13	0.87	271.33	6.08	56.59	59.51	34.34	36.11
1985	267.1	−3.476	264.93	3.37	54.15	57.99	32.86	35.19
1986	276.24	−0.173	267.56	4.61	56	58.69	33.98	35.61
1987	275.4	−0.477	258.03	0.88	55.83	56.39	33.88	34.34
1988	270.21	−2.428	279.77	9.38	54.74	61.36	33.21	37.23
1989	283.35	2.395	261.99	2.43	57.45	57.46	34.86	34.87
1990	279.64	1.055	251.04	−1.85	56.69	55.06	34.4	33.41
1991	283.3	2.348	254.01	−0.69	57.42	55.71	34.84	33.81
1992	275.74	0.058	250.08	−1.95	56.13	55	34.06	33.38
1993	265.63	−4.911	251.29	−1.76	53.35	55.11	32.37	33.44
1994	277.33	−0.852	233.57	−8.68	55.62	51.23	33.75	31.09
1995	273.8	1.005	237.84	−7.01	55.53	52.17	33.7	31.65
1996	270.22	−2.348	242.1	−5.35	54.78	53.1	33.24	32.22
1997	275.87	−0.307	252.6	−1.24	55.93	55.4	33.93	33.62
1998	278.16	0.513	227.91	−10.89	56.39	49.99	34.21	30.33
1999	272.39	−1.568	228.39	−10.71	55.22	50.09	33.51	30.39
2000	276.11	−0.22	236.13	−7.68	55.98	51.79	33.97	31.43
2001	278.42	0.614	227.81	−10.94	56.45	49.96	34.25	30.32
2002	270.95	−2.085	253.04	−1.07	54.93	55.5	33.33	33.68
2003	277.45	0.263	226.09	−11.37	56.23	49.72	34.13	30.17
2004	296.7	−2.54	234.09	−8.36	54.68	51.4	33.18	31.19
2005	274.22	−0.907	227.81	−10.94	55.59	49.96	33.73	30.32

Table 3. *Seasonal variation of intensity of OH(8, 3) from 1979–2005 at New Delhi.*

Year	Amount of O_3(DU) in winter	O_3 fluctuation % from mean in winter	Intensity of OH(8, 3) in winter KR	Amount of O_3 (DU) in pre-monsoon	O_3 fluctuation % from mean in pre-monsoon	Intensity of OH(8, 3) in pre-monsoon KR	Amount of O_3 (DU) in monsoon	O_3 fluctuation % from mean in monsoon	Intensity of OH(8, 3) in monsoon KR	Amount of O_3 (DU) in post-monsoon	O_3 fluctuation % from mean in post-monsoon	Intensity of OH(8, 3) in post-monsoon KR
1979	290.33	7.29	36.52	299.8	4.31	35.51	287.86	2.35	34.84	273.24	2.3	34.82
1980	270.95	0.13	34.08	292.46	1.76	34.64	284.27	1.07	34.4	272.78	2.13	34.77
1981	284.84	5.27	35.83	296.46	3.16	35.12	283.2	0.69	34.27	275.93	3.31	35.17
1982	282.59	4.43	35.55	310.88	8.17	36.82	292.17	3.35	35.24	273.11	2.25	34.8
1983	274.61	1.49	34.55	281.68	−1.99	33.36	282.13	0.38	34.16	268.56	0.55	34.23
1984	285.28	5.43	35.89	287.25	−0.05	34.02	281.9	0.23	34.12	262.07	−1.88	33.4
1985	259.69	−4.03	32.67	269.19	−6.33	31.88	272.77	−3.02	32.95	266.74	0.13	34.08
1986	274.01	1.26	34.47	288.13	0.26	34.13	274.94	−2.23	32.28	267.86	0.28	34.14
1987	263.21	−2.73	33.11	293.21	2.03	34.73	283.94	0.96	34.37	261.13	−2.67	33.13
1988	269.61	−0.36	33.92	272.29	−5.24	32.26	273.93	−2.59	33.16	264.99	0.79	34.31
1989	279.51	3.3	35.16	290.6	1.17	34.44	286.78	1.97	34.71	272.99	2.21	34.79
1990	277.43	3.21	35.13	289.23	0.64	34.25	280.32	−0.33	33.93	271.58	1.67	34.61
1991	275.78	1.92	34.69	297.21	3.42	35.2	286.87	1.88	34.68	273.33	2.33	34.83
1992	267.14	−1.27	33.61	291.94	1.6	34.58	280.46	1.34	34.5	263.43	1.37	34.51
1993	256.55	−5.19	32.27	274.43	−4.51	32.5	273.77	−2.66	33.13	257.97	3.42	35.2
1994	276.54	5.6	35.95	287.48	0.03	34.05	277.75	−1.24	33.62	267.55	0.17	34.1
1995	267.78	−1.04	33.69	287.33	−0.02	34.03	276.53	−1.68	33.477	263.54	−1.33	33.59
1996	259.03	−4.27	32.59	286.52	−0.03	33.94	275.32	−2.11	33.32	260.02	−2.65	33.14
1997	265.15	−2.01	33.36	285.72	−0.58	33.84	278.48	−0.98	33.71	274.13	2.63	34.93
1998	270.86	3.39	35.19	290.17	0.97	34.37	283.15	0.68	34.27	263.74	−1.26	33.61
1999	263.18	−2.73	33.11	268.56	−6.55	31.81	283.75	0.89	34.34	274.06	2.61	34.93
2000	268.55	−0.75	33.78	289.65	0.79	34.31	284.98	1.33	34.49	261.25	−2.19	33.29
2001	265.92	−1.72	33.45	296.57	3.19	35.13	284.59	1.19	34.45	266.44	−0.25	33.95
2002	258.96	−2.05	33.34	276.89	−3.65	32.79	278.68	−0.91	33.37	269.26	0.81	34.32
2003	276.65	2.24	34.8	288.89	0.52	34.22	282.28	0.36	34.16	261.99	1.91	34.69
2004	257.8	−4.73	32.43	276.8	−3.68	32.78	280.51	−0.26	33.95	263.68	−1.28	33.6
2005	263.96	−2.45	33.21	290.11	0.95	34.36	282.49	0.44	34.19	260.29	−2.51	33.19

Table 4. *Seasonal variation of intensity of OH (8, 3) from 1979–2005 at Halley Bay.*

Year	Amount of O_3 (DU) in Summer	O_3 fluctuation % from mean in Summer	Intensity of OH(8, 3) in Summer KR	Amount of O_3 (DU) in Fall	O_3 fluctuation % from mean in Fall	Intensity of OH(8, 3) in Fall KR	Amount of O_3 (DU) in Winter	O_3 fluctuation % from mean Winter	Intensity of OH(8, 3) in Winter KR	Amount of O_3 (DU) in Spring	O_3 fluctuation % from mean in Spring	Intensity of OH(8, 3) in Spring KR
1979	320.19	8.43	36.88	293.79	8.24	36.84	289.61	17.66	40.05	298.58	41.95	48.32
1980	332.7	12.66	38.35	299.26	10.26	37.53	290.15	17.88	40.13	275.82	31.04	44.73
1981	325.95	10.37	37.57	279.5	2.98	35.05	289.03	17.43	39.97	285.29	35.54	46.14
1982	314.14	6.38	36.21	287.37	5.88	36.04	289.93	17.8	40.1	259.11	23.1	41.9
1983	326.53	10.57	37.64	287.7	2.68	34.95	272.82	10.84	37.73	259.2	23.14	41.92
1984	311.3	5.41	35.88	278.83	2.73	34.97	265.78	7.98	36.76	229.42	8.99	37.1
1985	302.05	2.43	34.87	275.28	1.42	34.52	259.28	5.34	35.86	220.94	4.96	35.73
1986	298.94	1.23	34.46	251.98	−7.16	31.36	264.22	7.35	36.54	255.11	21.98	41.52
1987	297.21	0.64	34.26	280.33	3.28	35.16	262.08	6.48	36.25	192.49	8.55	36.95
1988	308.26	4.39	35.53	279.08	2.82	34.99	268.19	8.96	37.09	263.53	25.2	42.62
1989	299.85	1.54	34.56	275.21	1.4	34.52	254.2	3.28	35.16	218.68	3.89	35.36
1990	284.85	3.54	35.25	269.34	−0.76	33.78	243.29	−1.15	33.65	206.65	−1.82	33.42
1991	300.78	1.85	34.67	263.16	−3.04	33.01	238.32	−3.17	32.96	213.78	1.56	34.57
1992	295.53	0.07	34.06	278.78	2.71	34.96	238.9	2.94	35.04	189.92	−9.77	30.71
1993	296.48	0.4	34.18	277.4	2.2	34.79	252.88	2.74	34.97	178.39	−15.25	28.85
1994	288.29	−2.38	33.23	274.28	1.05	34.4	205.51	−16.5	28.42	166.21	−21.03	26.88
1995	288.35	−2.36	33.24	272.53	0.41	34.18	218.87	−11.08	30.27	171.59	18.49	40.33
1996	288.41	−2.34	33.24	270.81	−0.22	33.97	232.23	5.65	35.96	176.97	−15.92	28.62
1997	299.52	1.43	34.53	269.05	−0.87	33.74	251.58	2.21	34.08	190.04	−9.72	30.73
1998	253.5	−14.16	29.22	269.99	−0.52	33.86	229.3	−6.84	31.71	158.87	−24.52	25.69
1999	262.71	11.03	37.79	263.66	−2.86	33.07	231.53	−5.93	32.02	155.67	−26.04	25.18
2000	284.39	3.7	35.19	260.69	−3.95	32.7	221.46	−10.02	30.57	177.97	−15.45	28.78
2001	273.54	−7.37	31.53	258.77	−4.66	32.45	216.99	−11.84	30.01	161.92	−23.07	26.19
2002	286.13	−3.11	32.98	256.13	−5.6	32.14	226.34	8.04	36.78	243.56	15.71	39.39
2003	284.01	3.83	35.34	252.16	−7.1	31.62	198.6	19.31	40.6	171.98	−18.3	27.81
2004	278.74	−5.61	32.28	251.14	−7.47	31.5	224.36	−8.84	31.03	183.32	−12.91	29.65
2005	270.89	−8.27	31.22	252.1	−7.12	31.62	210.03	−14.67	29.05	178.21	−15.34	28.82

inter-annual changes of dynamical structure in the lower stratosphere and contemporaneous changes of ozone observed by TOMS, Salby *et al.* (2002) also concluded that inter-annual changes of ozone in the lower stratosphere is accompanied by coherent changes of ozone in the upper stratosphere and mesosphere. Increase in stratospheric ozone will enhance the mesospheric ozone through vertical transport of more ozone, whereas the decrease in stratospheric ozone will accompany with less transport of ozone into the mesosphere through diffusion because of low density of ozone. Consequently, the mesospheric ozone density will decrease (Jana *et al.* 2011). Percentage of ozone fluctuation for each year has been calculated from the mean of the yearly mean concentration of ozone during the period 1979–2005. The effect of variation of ozone has been considered in the calculation of volume emission rate and intensities of OH(8, 3) band since it is proportional to the atomic oxygen as well as molecular oxygen densities, assuming that the concentrations of atomic hydrogen remain constant, because it influences the production of OH nightglow in one hand and it destructs the ozone in other hand which in turn reduces the production of OH.

The mean of the yearly mean values of ozone concentrations during the period 1979–2005 for the stations New Delhi and Halley Bay were 263.92 and 255.78 DU, respectively. Then percentages of variation of O_3 concentration from its mean have been computed for different years and are shown in table 2. These were 2.35% and 17.5% for the year 1979 for New Delhi and Halley Bay, respectively. During this year altitudinal concentrations of ozone, volume emission rates and intensities of OH(8, 3) band were enhanced by 2.35% and 17.5% at New Delhi and Halley Bay, respectively, as shown in table 1. The altitudinal variations of volume emission rate for New Delhi and Halley Bay have been shown in figure 1. Intensities were 34.84 and 39.99 KR at New Delhi and Halley Bay, respectively, for the year 1979.

Following this procedure, the intensities for different years and seasons have been calculated for the period 1979 to 2005 and are shown in tables 2–4 for these two stations. The yearly variations of intensities have been shown in figure 6. Figure 6 indicates that the rates of decrease of intensities at New Delhi and Halley Bay were 0.0269 and 0.3571 KR per year, respectively. Intensities of OH(8, 3) for seasons winter, pre-monsoon, monsoon and post-monsoon over New Delhi and summer, fall, winter and spring over Halley Bay been computed for the same period are shown in tables 3 and 4, respectively. The variations of seasonal intensities over New Delhi and Halley Bay have been depicted in figures 7 and 8, respectively. It has been observed that in all seasons over these two

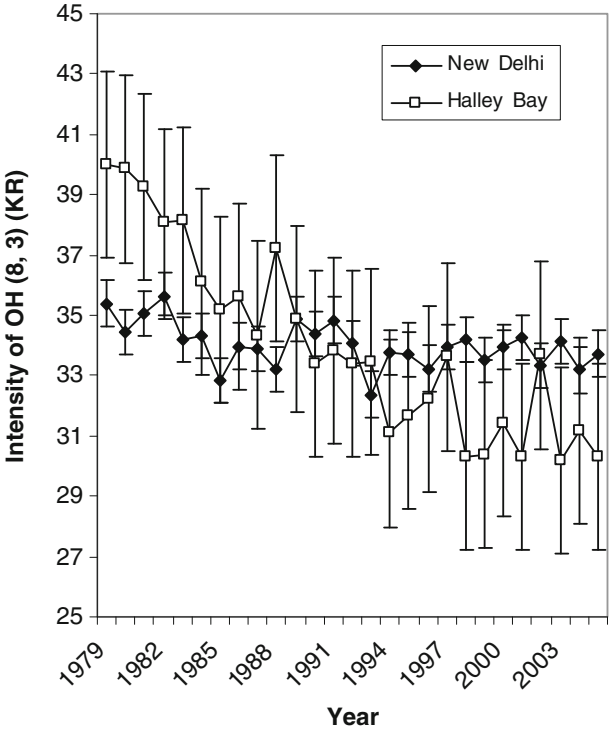

Figure 6. Yearly variations of intensity of OH(8, 3) band at New Delhi (29°N, 77°E) and at Halley Bay (76°S, 27°W) from 1979 to 2005.

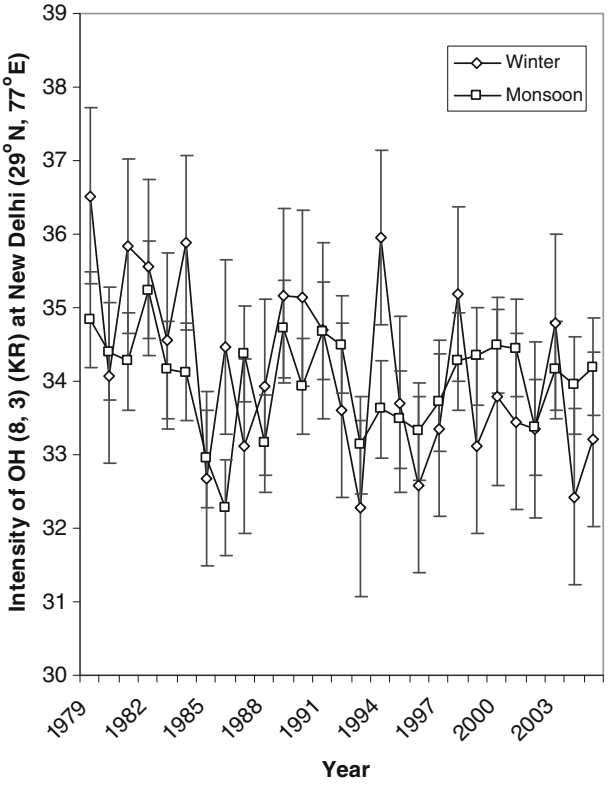

Figure 7. Seasonal variations of intensity of OH(8, 3) band at New Delhi (29°N, 77°E) from 1979 to 2005.

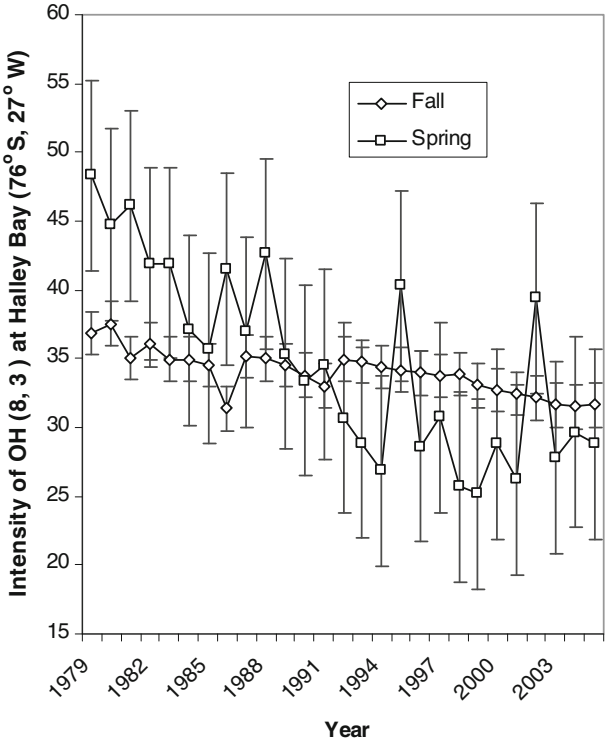

Figure 8. Seasonal variations of intensity of OH(8, 3) at Halley Bay (76°S, 27°W) from 1979 to 2005.

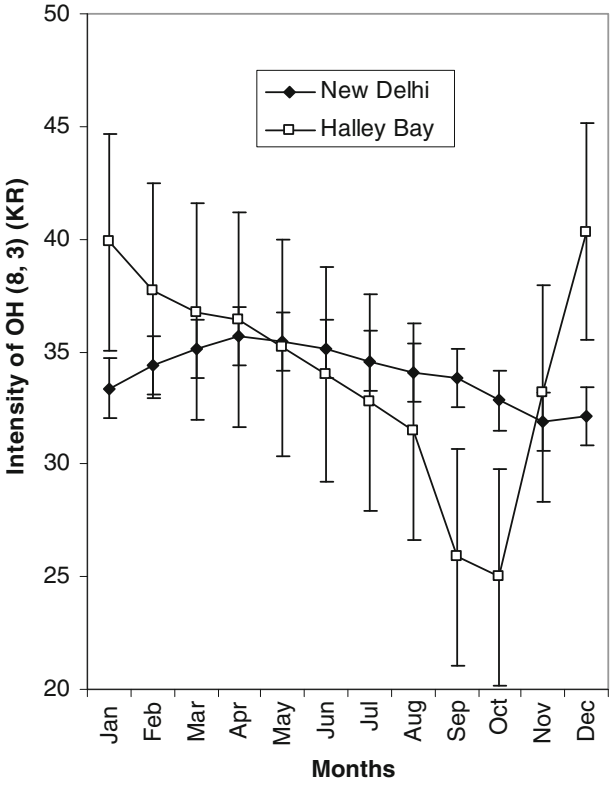

Figure 9. Mean annual cycle of intensity of OH(8, 3) band at New Delhi (29°N, 77°E) and at Halley Bay (76°S, 27°W).

stations, the intensity had declined from 1979 to 2005 with different rates. The maximum rate of intensity depletion was noticed in winter (0.0763 KR/year) and spring (0.6893 KR/year) over New Delhi and Halley Bay, respectively because of the maximum ozone fall; but the minimum rate of intensity depletion was seen in monsoon (0.0092 KR/year) and fall (0.1559 KR/year) due to the minimum ozone decline during these seasons, respectively. Again, all rates of yearly as well as all seasonal intensity decline over Halley Bay were much higher than that over New Delhi.

The mean of monthly mean ozone concentration for each month during 1979–2005 has been calculated and are shown in table 5. Percentages of ozone fluctuation from the mean of January to December ozone values have been calculated for these stations. The intensities of OH(8, 3) band have then been calculated considering the

Table 5. *Annual cycles of intensity of OH(8, 3) line at New Delhi and Halley Bay.*

Months	Mean O_3 (DU) at New Delhi	O_3 fluctuation % from mean at New Delhi	Intensity of OH(8, 3) line at New Delhi KR	Mean O_3 (DU) at Halley Bay	O_3 fluctuation % from mean at Halley Bay	Intensity of OH(8, 3) line at Halley Bay KR
January	271.45	−1.94	33.38	299.54	17.11	39.86
February	279.39	0.97	34.37	283.52	10.77	37.71
March	285.61	3.22	35.14	276.26	8	36.76
April	290.1	4.84	35.69	273.57	6.96	36.41
May	287.97	4.07	35.43	264.43	3.38	35.19
June	285.48	3.17	35.12	255.29	−0.19	33.98
July	281.22	1.63	34.59	246.15	−3.76	32.76
August	277.09	0.14	34.09	236.31	−7.61	31.45
September	275	−0.62	33.83	194.43	−23.98	25.88
October	266.78	−3.59	32.82	187.87	26.55	25
November	259.49	−6.22	31.92	249.16	−2.59	33.16
December	260.91	−5.71	32.1	303.05	18.58	40.33

corresponding ozone fluctuation percentages. The variations of intensities for different months in a year for these two stations have been shown in figure 9 which clearly indicates the maximum intensities in the month of June for New Delhi and December and January for the Halley Bay station, whereas, the minimum intensities in the month of January and October over these two stations respectively.

4. Conclusions

The yearly variations of TCO concentration in DU at New Delhi and Halley Bay were mainly controlled by their August and September concentrations, respectively, because the nature of August and September ozone variations was the most identical with that of yearly ozone variations over these two stations, respectively, from 1979 to 2005 that was also testified by the variation of coefficient of correlation with all months. The rate of yearly mean TCO depletion from 1979 to 2005 was the closest to that of monthly mean TCO fall during the month of August over New Delhi while, the rate of yearly mean TCO depletion from 1979 to 2005 was the closest to that of monthly mean TCO decline during the month of September over Halley Bay for the same period. Moreover, the rate of intense depletion of TCO during the month of September over Halley Bay from 1979 to 2005 contributed more than that of any other month to the yearly TCO depletion. During the month of August, the rate of ozone depletion catalyzed by various ozone depleting substances was more than that of ozone formation processes and was also comparable to the rate of yearly decline of ozone over New Delhi. During the month of September, the rate of ozone depletion catalyzed by various ozone depleting substances was much more than that of ozone formation processes and was also comparable to the rate of yearly decline of ozone over Halley Bay. Whereas, seasonal variations of TCO shows that winter variation at New Delhi and spring time variation of ozone over Halley Bay were the most identical with their yearly mean variation of ozone from 1979 to 2005. The rate of ozone depletion at Halley Bay was comparatively higher than that at New Delhi and attained maximum during September to October at Halley Bay due to predominant ozone decline processes caused by lower temperature of about -80°C, larger concentrations of Cl and ClO radicals and appearance of more polar stratospheric clouds (PSCs) at Halley Bay.

OH airglow emissions as tracers of gravity wave (GW) play an essential role in determining the global circulation and thermal balance of the atmosphere. A realistic GW parameterization is important for accurate atmospheric model. Dynamic control of OH altitude/temperature at high latitudes was supported by the anti-correlation between OH peak altitude and temperature found in SABER data and also between OH peak altitude and meridional wind strength. Influence of variation of total column ozone on OH airglow emission is an important approach for investigating the coupling between stratosphere and mesosphere-lower thermosphere (MLT) regions. The densities of atomic oxygen, hydrogen and rotational temperature can also be calculated from OH airglow emission and known concentration of ozone at mesospheric region.

The volume emission rate of OH(8, 3) band attained maximum at an altitude of 80 km, due to the maximum value of the product of $n(O_3)$ and n(H). The volume emission rate and intensity of OH(8, 3) band at Halley Bay (76°S, 27°W) were comparatively higher than that at New Delhi in 1979 due to its higher percentage of ozone increase from its mean value. The yearly and seasonal intensities of OH(8, 3) gradually decreased from 1979 to 2005 at both the stations with different rates. The decline in intensity occurred maximum during winter and spring over New Delhi and Halley Bay, respectively due to larger loss of TCO; but the minimum decline in intensity had attained during monsoon and fall over these two stations, respectively because of less ozone depletion. The rate of both the yearly and seasonal decrease in intensity was greater at Halley Bay due to much larger loss rate of yearly mean and seasonal mean ozone concentration from 1979 to 2005. The coefficient of correlation between yearly mean and seasonal mean intensities was the maximum (0.79) for winter in case of New Delhi and for spring (0.9) in case of Halley Bay; since the nature of winter and spring variations in intensities of OH(8, 3) was the most identical with that of the yearly mean variation over New Delhi and Halley Bay, respectively for the period 1979–2005.

The mean annual cycle of intensities of OH(8, 3) band for the stations New Delhi and Halley Bay represented in figure 8 clearly reveals that maximum intensity of OH(8, 3) band occurred for the month of June for the greater concentration of ozone and minimum intensity occurred for the month of January for the less concentration of ozone at New Delhi, but in case of Halley Bay, maximum intensity occurred during the month of December due to higher concentration of ozone and minimum intensity occurred for the month of September because of the less concentration of ozone. Intensity of OH(8, 3) band gradually increased from the month of January, attained its maximum for the period of June and July and then

gradually decreased at New Delhi. But for Halley Bay, maximum intensity of OH(8, 3) band occurred for the month of December and January, then intensity gradually decreased, attained minimum for the month of September, then intensity gradually increased. The minimum intensity of OH(8, 3) band during the month of September at Halley Bay was due to the dramatic decrease in ozone concentration at Halley Bay during spring time because of special atmospheric climatic condition at Antarctica during spring time.

References

Abreu V J and Yee J H 1989 Diurnal and seasonal variation of the nighttime OH(8, 3) emission at low latitudes; *J. Geophys. Res.* **94(A9)** 11,949–11,957.

Bates D R and Nicolet M 1950 The photochemistry of atmospheric water vapour; *J. Geophys. Res.* **55(3)** 301–327.

Batista P P, Takahashi H and Clemesha B R 1994 Solar cycle and the QBO effect on the mesospheric temperature and night glow emissions at a low latitude station; *Adv. Space Res.* **14(9)** 221–224.

Bittner M, Offermann D and Graef H 2000 Mesopause temperature variability above a midlatitude station in Europe; *J. Geophys. Res.* **105(D2)** 2045–2058.

Bodeker G E, Struthers H and Connor B G 2002 Dynamical containment of Antarctic ozone depletion; *Geophys. Res. Lett.* **29** 14,206.

Bojkov R D 1992 Scientific assessment of ozone depletion; *WMO Bulletin* **41** 171.

Breig E L 1970 Secondary production process for the hydroxyl atmospheric airglow; *Planet. Space Sci.* **18** 1271.

Cordero E C and Nathan T R 2002 An examination of anomalously low column ozone in southern hemisphere mid-latitude during 1997; *Geophys. Res. Lett.* **29** 1123, doi: 10.1029/2001GL013948.

deMesnes F C, Shiguemori E H, Muralikrishna P and Clemesha B R 2011 A representative airglow volume emission profile from rocket-borne photometer data by an artificial neural network technique; *J. Comput. Interdisciplinary Sci.* **2(2)** 99–109.

Dyrland M E, Mulligan F J, Hall C M, Sigernes F, Tsutsumi M and Deehr C S 2010 Response of OH airglow temperatures to neutral air dynamics at 78°N, 16°E during the anomalous 2003–2004 winter; *J. Geophys. Res.* **115** D07103, doi: 10.1029/2009JD012726.

Farman J C, Gardiner B G and Shanklin J D 1985 Large losses of total ozone in Antarctica reveal seasonal ClO_x/NO_x interaction; *Nature* **315** 207–210.

Funke B, Lopez-Puertas M, Bermejo-Pantaleon D, Garcia-Comas M, Stiller G P, vonClarmann T, Kiefer M and Linden A 2010 Evidence for dynamical coupling from the lower atmosphere to the thermosphere during a major stratospheric warming; *Geophys. Res. Lett.* **37** L13803, doi: 10.1029/2010GL043619.

Gao H, Xu J and Wu Q 2010 Seasonal and QBO variations in the OH nightglow emission observed by TIMED/SABER; *J. Geophys. Res.* **115** A06313, doi: 10.1029/2009JA014641.

Gao H, Xu J, Ward W and Smith A K 2011 Temporal evolution of nightglow emission responses to SSW events observed by TIMED/SABER; *J. Geophys. Res.* **116** D19110, doi: 10.1029/2011JD015936.

Gattinger R L 1971 *The Radiation Atmosphere* (ed.) McCormac B M (Dordrecht: D. Reidel), 51p.

Gombosi T I 2004 *Physics of the Space Environment*; Cambridge University Press.

Greet P A, French W J R, Burns G B, Williams P F B, Lowe R P and Finlayson K 1998 OH(6-2) spectra and rotational temperature measurements at Davis, Antarctica; *Ann. Geophys.* **16(1)** 77–89.

Haider S A, Kim J, Nagy A F, Kellere N, Verigin M I, Gringauz K I, Shutte N M, Szego K and Kiraly P 1992 Calculated ionization rates, ion densities and airglow emission rates due to precipitating electrons in the night side ionosphere of Mars; *J. Geophys. Res.* **97** 10,637–10,641.

Hargreaves J K 1992 *The Solar-Terrestrial Environment*; Cambridge University Press.

Jacchia L G 1977 SAO Special Report No. 375, Smithsonian Institution Astrophysical Observatory, Cambridge, Massachusetts.

Jana P K and Nandi S C 2005 Effect of solar parameters on Antarctic, artic and tropical ozone during the last solar cycle; Indian *J. Radio Space Phys.* **34** 114–118.

Jana P K and Nandi S C 2006 Ozone decline and its effect on night airglow intensity of Na 5893 Å at Dumdum (22.5°N, 88.5°E) and Halley Bay (76°S, 27° W); *J. Earth Syst. Sci.* **115** 607–613.

Jana P K, Saha I, Das P, Sarkar D and Midya S K 2010a Long-term ozone trend and its effect on night airglow intensity of Li 6708 Å at Ahmedabad (23°N, 72.5°E) and Halley Bay (76°S, 27°W); *Indian J. Phys.* **84(1)** 41–53.

Jana P K, Saha D K and Midya S K 2010b Effect of cloud on atmospheric ozone formation over Kolkata; *Indian J. Phys.* **84(4)** 367–375.

Jana P K, Saha I and Mukhopadhyay S 2011 Long-term ozone decline and its effect on night airglow intensity of Li 6708 at Varanasi (25°N, 83°E) and Halley Bay (76°S, 27°W); *J. Earth Syst. Sci.* **120(2)** 291–300.

Jana P K, Sarkar D, Saha D K and Midya S K 2012 Effect of cloud occurrences on tropospheric ozone over Alipore (22.52°N, 88.33°E); *J. Earth Syst. Sci.* **121(3)** 711–722.

Kerr A 1998 Deep chill triggers record ozone hole; *Science* **282** 391.

Krasnopolsky V A 1986 Oxygen emissions in the night airglow of the earth, Venus and Mars; *Planet. Space Sci.* **34(6)** 511–518.

Krassovsky V J 1956 *On the Detection of the Infra-red Night Airglow and Aurrora* (eds) Armstrong S B and Dalgarno A (New York, USA: Pargamon Press), 193p.

Krassovsky V I and Shagaev M V 1974 Inhomogeneties and wavelike variations of the rotational temperature of atmospheric hydroxyl; *Planet. Space Sci.* **22** 1334–1337.

Llewellyn E J, Long B H and Solheim B H 1978 The quenching of OH* in the atmosphere; *Planet. Space Sci.* **26** 525–531.

Lowe R P and Turnbull O N 1995 Comparison of ALOHA-93, ANLC-03 and ALOHA-90 observations of the hydroxyl rotational temperature and gravity wave activity; *Geophys. Res. Lett.* **22** 2813–2816.

Madrigal M A and Peraza J P 2005 Analysis of the evolution of the Antarctic ozone hole size; *J. Geophys. Res.* **110** D02107, doi: 10.1029/2004JD004944.

Meinel A B 1950a Hydride emission bands in the spectrum of the night sky; *J. Astrophys.* **111** 207.

Meinel A B 1950b OH emission bands in the spectrum of the night sky, I; *J. Astrophys.* **111** 555–564.

Meinel A B 1950c OH emission bands in the spectrum of the night sky, II; *J. Astrophys.* **112** 120–130.

Marcos F A 1987 Proceedings of workshop held at AFGC on atmospheric density and aerodynamics drag models for air force operations.

Marsh D R, Smith A K, Mlynczak M G and Russell III J M 2006 SABER observations of the OH Meinel airglow variability near the mesopause; *J. Geophys. Res.* **111** A10S05, doi: 10.1029/2005JA011451.

Midya S K and Jana P K 2002 Atmospheric ozone depletion and its effect on environment; *Indian J. Phys.* **76B** 107–138.

Midya S K, Jana P K and Mondal S K 1998 OH(8, 3) band emission from different excitation mechanisms; *Indian J. Phys.* **72B(5)** 547–553.

Midya S K and Midya D 1993 The effect of Antarctic O_3 decline on night airglow intensity of Na 5893 Å , O5577 Å, OH emissions and its correlation with solar flare numbers; *Earth, Moon & Planets* **61** 175–182.

Mlynczak M G, Zhou D K and Alder-Golden S M 1998 Kinetic and spectroscopic requirements for the inference of chemical heating rates and atomic hydrogen densities from OH Meinel band measurements; *Geophys. Res. Lett.* **25** 647–650.

Nelson D D, Schiffman Jr. A, Nesbitt D J, Orland J J and Burkholder J B 1990 H + O_3 → Fourier transform infrared emission and laser absorption studies of OH($X^2\pi$) radical: An experimental dipole moment function and state-to-state, Einstein A coefficients; *J. Chem. Phys.* **93** 7003–7019.

Nicolet M 1970 Ozone and hydrogen reactions; *Ann. Geophys.* **26** 531–546.

Salby M, Callaghan P, Keckhut P, Godin S and Guirlet M 2002 International changes of temperature and ozone, relationship between the lower and upper stratosphere; *J. Geophys. Res.* **107(D18)**, doi: 10.1029/2001 JD000421.

Sathiskumar S and Sridharan S 2009 Planetary and gravity waves in the mesosphere and lower thermosphere region over Tirunalveli (8.7°N, 77.8°E) during stratospheric warming events; *Geophys. Res. Lett.* **36** L07806, doi: 10.1029/2008GL037081.

Shephered M G, Liu G and Shephered G G 2006 Mesospheric semiannual oscillation in temperature and nightglow emission; *J. Atmos. Sol. Terr. Phys.* **68(3–5)** 379–389.

Slanger T G, Cosby P C, Huestic D L and Bida T A 2001 Discovery of the atomic oxygen green line in the Venus night airglow; *Science* **291** 463–465.

Stuhl F and Niki H 1971 Measurement of rate constants for termolecular reactions O(3P) with NO, O_2, CO, N_2 and CO_2 using a pulsed vaccum-uv photolysis-chemiluminescent method; *J. Chem. Phys.* **55** 3943–3953.

Takahashi H, Clemesha B R and Sahai Y 1974 Nightglow OH(8, 3) band intensities and rotational temperature at 23°S; *Planet. Space Sci.* **22** 1323–1329.

Takahashi H, Sahai Y, Clemesha B R, Batista P P and Teixeira N R 1977 Diurnal and seasonal variation of the OH(8, 3) airglow band and its correlation with OI 5577 Å; *Planet. Space Sci.* **25** 541–547.

Uchino O, Bojkov R, Balis D S, Akagi K, Hayashi M and Kajihara R K 1999 Essential characteristics of the Antarctic spring ozone decline: Update to 1998; *Geophys. Res. Lett.* **26** 1377–1380.

Ward W E 1999 A simple model of diurnal variations in the mesospheric oxygen nightglow; *Geophys. Res. Lett.* **26(23)** 3565–3568.

Wrasse C M, Takahashi H and Gobbi D 2004 Comparison of the OH (8-3) and (6-2) band rotational temperature of the mesospheric airglow emissions; *Rev. Bras. Geof.* **22(3)** 223–231.

Wiens R H and Weill G 1973 Diurnal, annual and solar cycle variations of hydroxyl and sodium nightglow intensities in the Europe–Africa sector; *Planet. Space Sci.* **21** 1011–1027.

Winick J R, Wintersteiner P P, Picard R H, Esplin D, Mlynczak M G, Russell III J M and Gordley L L 2009 OH layer characteristics during unusual boreal winters of 2004 and 2006; *J. Geophys. Res.* **114** A02303, doi: 10.1029/2001 JA013688.

World Meteorological Organization (WMO) 2002 Scientific assessment of ozone depletion.

Xu J, Smith A K, Jiang G, Gao H, Wei Y, Mlynczak M G and Russell III J M 2010 Strong longitudinal variations in the OH nightglow; *Geophys. Res. Lett.* **37** L21801, doi: 10.1029/2010GL043972.

MS received 15 January 2012; revised 3 April 2012; accepted 29 June 2012